

# Effect of Laser Scan Speed on Microstructure and Microhardness on Titanium Clad Magnesium



Kannan Ganesa Balamurugan and Muthukannan Duraiselvam

## 1 Introduction

Magnesium alloys are influencing various sectors due to their low density and better manufacturing characteristics [1]. The magnesium and its alloys have extensive usage in orthopedic applications due to their biocompatibility and similar modulus of elasticity with the natural bone [2]. Their inferior corrosion resistance of the magnesium limits their end usage [3]. Numerous surface modification techniques are utilized to retard the corrosion rates of the magnesium alloys, like laser treatment, ion implementation, friction stir processing and thermal spraying [4]. Additionally, the protective coating can be applied to the magnesium surfaces through thermal spraying and laser cladding routes. In recent years, laser cladding gains more attraction to apply the protective coatings on the metallic materials. The laser cladding significantly improves the tribological properties of the metallic materials [5]. Various researchers have been attempting laser cladding technique to enhance the tribological properties of the magnesium alloys. Zeqin et al. [6] investigated a composite coatings on AZ31B magnesium alloy by laser cladding. The results revealed that the coating had enhanced the tribological properties of the AZ31B magnesium alloy substrates. Huang et al. [7] fabricated zirconium-based coating on AZ91D magnesium by laser cladding. The corrosion resistance and wear resistance of the AZ91D magnesium alloy had been enhanced by the presence of zirconium oxide and zirconium aluminide in the coating. Gao et al. [8] laser clad Aluminum–Silicon on AZ91HP magnesium alloy. The results showed that the formation of multiple intermetallic particles like  $Mg_2Si$ ,  $Mg_{17}Al_{12}$ , and  $Mg_2Al_3$  showed higher hardness, improved the tribological properties. However, the hardness of the coated magnesium alloys was higher than their

---

K. G. Balamurugan (✉)

IFET College of Engineering, Villupuram, Tamil Nadu 605108, India

M. Duraiselvam

National Institute of Technology Tiruchirappalli, Tiruchirappalli, Tamil Nadu 620015, India

uncoated counterparts. Even though the corrosion resistance of the coated magnesium alloys showed improvement than un-coated magnesium alloys; the results were not up to the expected level. There is a lack of literature regarding the Ti6Al4V cladding on pure magnesium. Therefore, the present work attempts the laser clad Ti6Al4V powder on pure magnesium substrate and aims to study its compatibility with the pure magnesium substrates by investigating through macrostructures and microstructures.

## 2 Experimental

Commercially pure magnesium with a dimension of  $30 \times 60 \times 10$  mm was used. The surfaces were polished with metallographic sandpapers and washed with alcohol. The Ti6Al4V powders with the average particle size of 60 microns were used as the coating material. The laser cladding on the magnesium substrate was carried out using the YB:YAG disk laser (solid-state laser), 4 kW capacity. The laser power of 600 watts and powder feed rate of 5 g/min were kept constant, and the laser scan speed was varied from 100 mm/min to 600 mm/min with the increment of 100 mm/min. The Ti6Al4V powders were coaxially fed into the molten pool of the substrate material, and the Argon was supplied at the rate of 10 L/min to protect the molten pool. Metallographic characterizations were carried out by cross-sectioned the laser clad specimens and polished to the silver finish. The Kroll's etchant was applied on the Ti6Al4V coating and Picral. Microhardness measurements were taken on the coating, interface and the substrate with the test load of 0.5 kg. The XRD analysis was performed at the cross-section of the clad substrates to identify the secondary phase particles formed due to laser cladding.

## 3 Results and Discussion

### 3.1 Ti6Al4V Clad Morphology with Magnesium Substrate

Figure 1 indicates the cross-section of the sample coated in 100 mm/min scan speed. Figure 1a reveals that coating has a large void present in the magnesium substrate near the interface. Microcracks were visible (Fig. 1a). Figure 1b shows the interface of the coating and the substrate. The interface indicated that the coating and the substrate were a metallurgically bonded. Formation of the oxide layer at the interface was evident from Fig. 1b. The micro-dimples were observed near the interface in the magnesium. Figure 2a shows the cross-section of the sample coated in 200 mm/min scan speed. Presence of microcracks was observed in the coating (Fig. 2b), and the metallurgical bonding was created between the substrate and the coating. Formation of the oxide layers was evident at the interface, and micro-dimples were also formed in the magnesium side near the interface (Fig. 2b). Figure 3a shows the cross-section

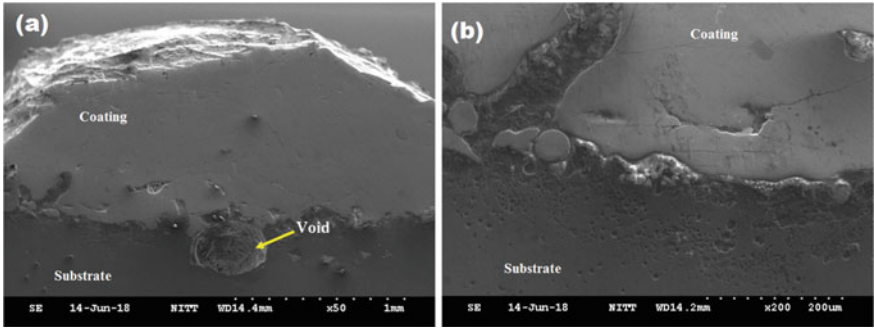


Fig. 1 SEM images of sample coated in 100 mm/min scan speed, a overall cross-section, b interface

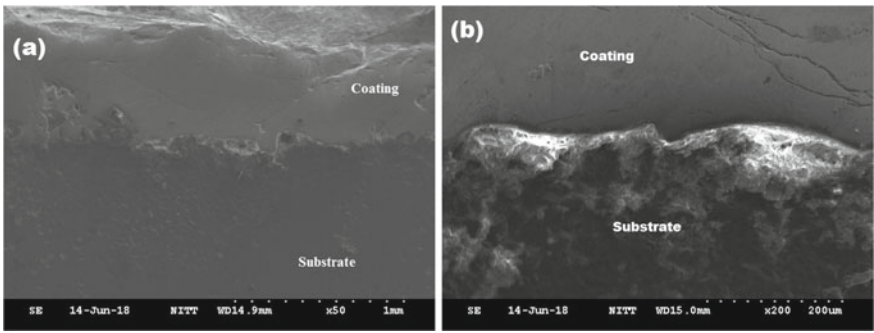


Fig. 2 SEM images of sample coated in 200 mm/min scan speed, a overall cross-section, b interface

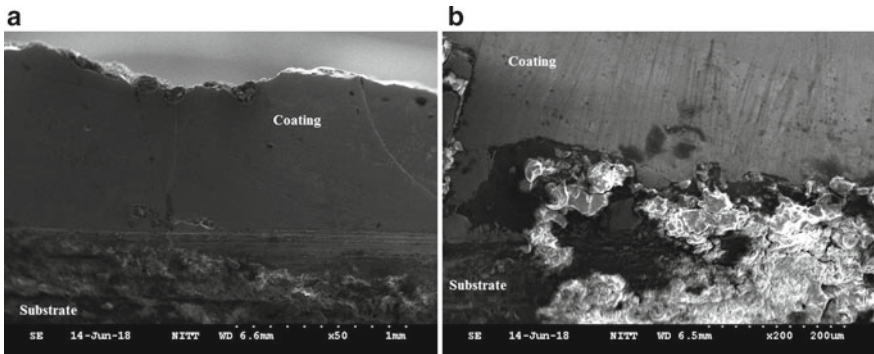
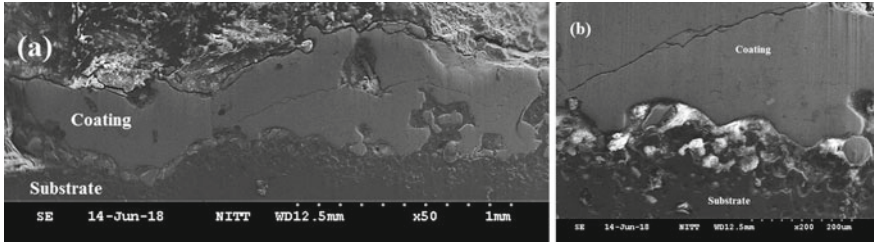
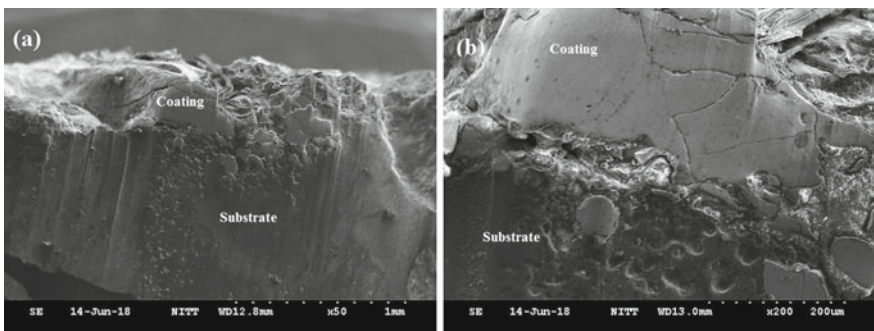


Fig. 3 SEM images of sample coated in 300 mm/min scan speed, a overall cross-section, b interface



**Fig. 4** SEM images of sample coated in 400 mm/min scan speed, **a** overall cross-section, **b** interface

of the sample coated in 300 mm/min scan speed. Figure 3a reveals that the formations of microcracks were minimum and the interface revealed a metallurgical bonding existed. Formation of oxide layer was also evident at the interface (Fig. 3b). Figure 4a shows the cross-section of the sample clad at 400 mm/min scan speed. Figure 4a indicates that the coating was not uniformly deposited and the presence of large cavities was observed. Figure 4b shows the formation of cracks in the coating. Like other samples, oxide layers were formed at the interface as evident from Fig. 4b. Insufficient coating formed at 500 and 600 mm/min scan speeds, as evident from the Figs. 5 and 6 Laser scan speed significantly affects the coating deposition on the magnesium substrate. Figures 1, 2, 3, 4, 5 and 6 indicate the deposition nature of the different scan speeds. The observations from the figures clarified that increased scan speed has resulted in unsatisfactory coating deposition. Especially in higher scan speeds like 500 and 600 mm/min, poor deposition has been resulted. The coating material was coaxially fed along with laser source and argon gas. The laser source melts the coating materials and forms the plume. The plume was focused on the surface of the magnesium substrate. When the high energy plume hits the substrate surface, it loses the energy and got solidified. This mechanism continues along the desired length on the substrate. The scan speed affects interacting period of the plume with the substrate. At lower scan speed, the plume has sufficient interaction time for the deposition and solidification. However, at the higher scan speed, the plume has



**Fig. 5** Sample coated in 500 mm/min scan speed, **a** overall cross-section, **b** interface

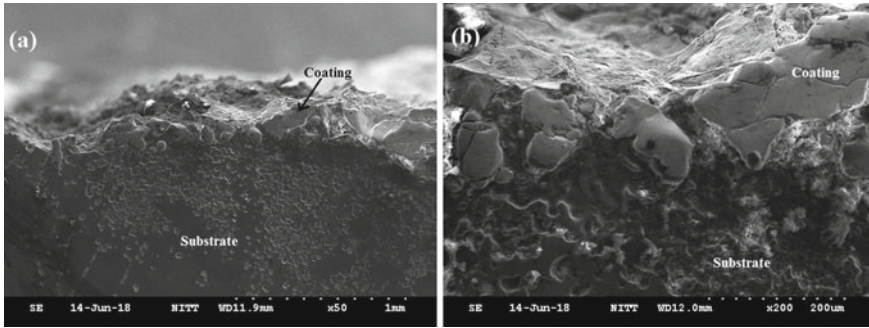


**Fig. 6** Sample coated in 600 mm/min scan speed, **a** overall cross-section, **b** interface

lower interaction time with the substrate which resulted in insufficient deposition and solidification. The substrate magnesium material was subjected to high irradiation in lower scan speed like 100 mm/min due to intense laser energy interaction which forms voids at the interface and cracks in the coating material (Fig. 1a).

### 3.2 Microstructure of the Ti6Al4V Clad Magnesium Substrates

Figure 7 shows the microstructures of the Ti6Al4V coating. Distinct grains were formed (Fig. 7a) and secondary phase particles were precipitated in their grain boundaries (Fig. 7b). During laser melting, the Ti6Al4V alloy powder attained beta transus temperature and rapidly solidified while hitting the surface of magnesium substrate. This rapid solidification yields various sizes of the grains and allows the some phases precipitated at grain boundaries. These precipitates form a dendritic structure at the

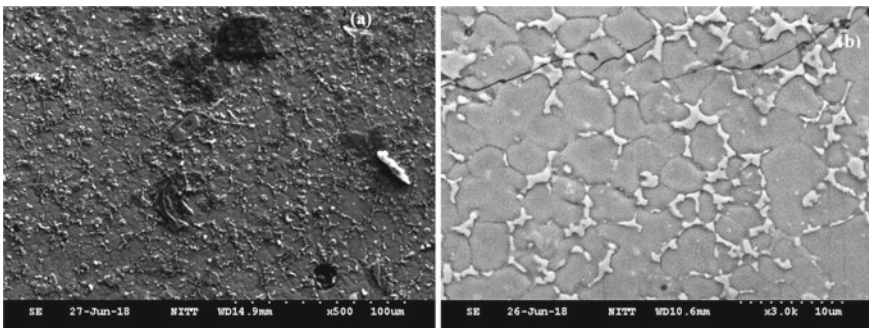


**Fig. 7** Microstructure of the Ti6Al4V coating, **a** lower magnification SEM image, **b** magnified SEM image



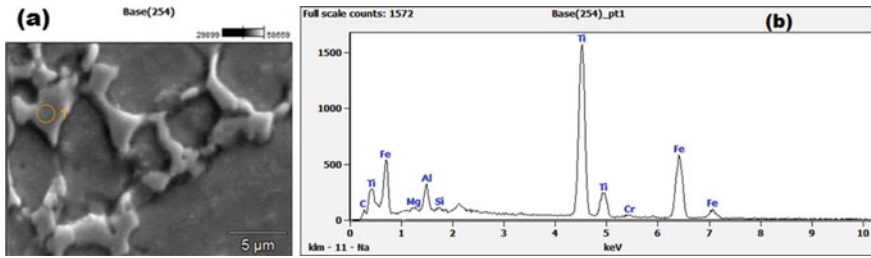


Fig. 8 a SEM image of the precipitate, b EDS result of the precipitate

grain boundaries. This phase contains  $\alpha + \beta$  platelet structure. This is the commonly forming phase in Ti6Al4V alloy [9]. Figure 8 shows the magnified image of the precipitate and the corresponding EDS result. The EDS result indicates that the precipitate contains the major elements of titanium, iron and aluminum and small traces of magnesium (Fig. 8b). During laser cladding process, considerable amount of magnesium substrate materials diffused in the titanium alloy matrix. The elemental mapping for cladding material proves the diffusion of magnesium substrate is significant (Fig. 9). Interface indicates the formation of oxide (Fig. 10a). EDS results ensure that the magnesium oxide is the constituent of this oxide layer (Fig. 10b). Elemental level diffusion occurred between Ti6Al4V coating and the magnesium substrate. However, substrate material shows higher diffusion in coating side than

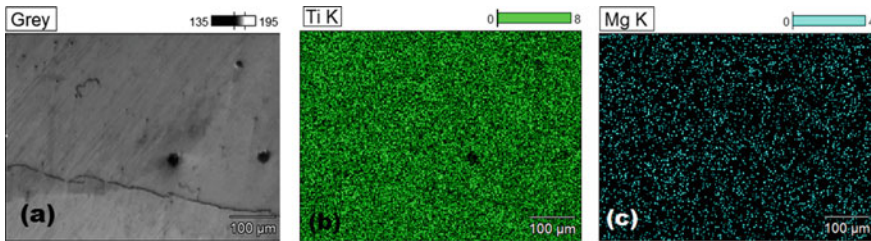


Fig. 9 Elemental mapping of Ti6Al4V coating, a SEM image of Ti6AlV4 coating, b Titanium elements in the coating, c Magnesium elements in the coating

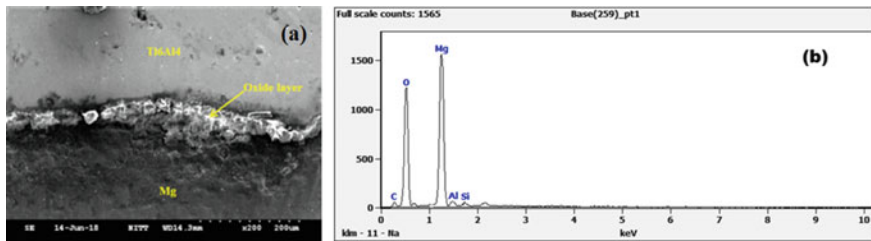
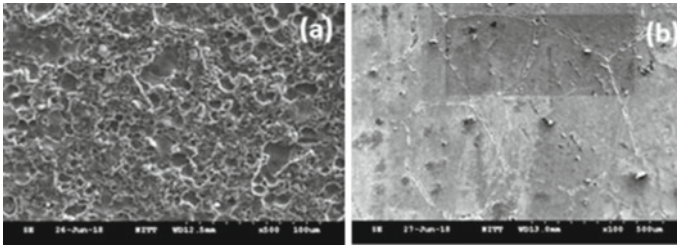


Fig. 10 a SEM image of the interface oxide layer, b EDS result of the oxide layer



**Fig. 11** a SEM image of heat affected zone of Ti6Al4V clad substrate, b Magnesium substrate microstructure

coating material into the substrate side as evident from the line scan. The magnesium substrate attained the melting temperature during the laser irradiation and diffused into the solidifying Ti6Al4V plume. The rate of solidification of Ti6Al4V plume was high compared to the magnesium substrate, thus the quantity of diffusion of magnesium into the coating material was high. Figure 11a shows the heat affected zone of Ti6Al4V clad magnesium substrate.

The heat affected zone of the magnesium contains network dendrites usually forms during laser treatment [10]. Figure 11b shows SEM image of magnesium substrate microstructure taken below the heat affected zone and the parent metal primary phase with large grains. The effect of heat input during laser cladding has no effect in this region. The laser scan speeds have less influence on the grain sizes and orientation of the coating and heat affected substrate. However, the scan speeds affect the intensities of intermetallic particles in the coating and heat affected substrate material. The intensities of the intermetallics vary with the scan speed. Figure 12 shows the XRD results of the laser clad specimens processed in various scan speeds. The XRD results revealed that the dominating intermetallic particles in the clad zones are  $Al_{12}Mg_{17}$ ,  $Fe_2O_3Ti$  and  $MgO$ . The  $Fe_2O_3Ti$  has been precipitated in the clad material and  $MgO$  has been precipitated in the interface (Fig. 10a). However,  $Al_{12}Mg_{17}$  has been resulted from the diffusion of substrate and coating materials on either side. Especially, due to the diffusion of magnesium into the coating side. The intensities of these intermetallic particles increasing while increasing the scanning speed (Fig. 12). At the higher scan speed, rapid heating and cooling of the coating and substrate material restricts the dissolution of the precipitated intermetallics into

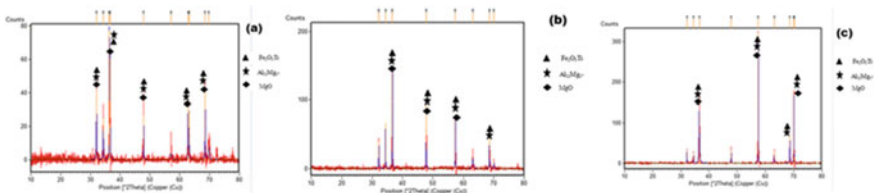
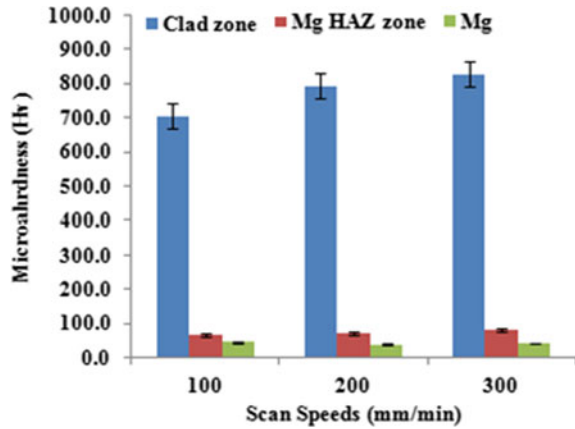


**Fig. 12** XRD results of Ti6Al4V clad samples at a 100 mm/min, b 200 mm/min, c 300 mm/min

**Fig. 13** Microhardness of the Ti6Al4V clad magnesium substrates at various scan speeds



their matrix. However, in case of lower scan speed, sufficient dissolution time was persisted.

### 3.3 Microhardness of Ti6Al4V Clad Magnesium Substrate

Figure 13 shows the microhardness of the Ti6Al4V clad magnesium substrates at various scan speeds. The microhardness result revealed that the clad zone has attained higher hardness than other zones like heat affected and non-heat affected magnesium substrate. Cladding zone shows ~95% higher microhardness than other zones. Similarly, heat affected zone shows ~44% increase than non-heat affected magnesium substrate. The intensities of the intermetallics present in the clad, HAZ zones influence the microhardness of the clad samples. Figure 13 indicates that the sample clad at 300 mm/min scan speed shows comparatively higher clad microhardness with higher intensity of intermetallics. The intermetallics are hard particles and offer resistance to indentation. Therefore, their increase in intensities increases the hardness of the clad specimens.

## 4 Conclusion

In this work, Ti6Al4V alloy was clad on pure magnesium substrate by laser cladding. The influence of laser scan speed on cladding morphology, microstructure and microhardness were investigated. Following conclusions were derived from this investigation.



- The optimum scan speed is identified as 300 mm/min. Increasing the laser scan speed above 300 mm/min resulted in inadequate coating deposition. However, at lower scan speeds, cracks and voids formed due to high interaction time of intense laser energy.
- The influence of laser scan speed on the grain size and their orientation was minimal in the clad and heat affected zones. However, it influences the intensities of intermetallic particles formed. The intensity of the intermetallics increase with increase in scan speed due to rapid solidification. The lower scan speed let the intermetallic particles to dissolve again into the matrix.
- Cladding zone shows ~95% higher microhardness than other zones and heat affected zone shows ~44% increase than non-heat affected magnesium substrate. Intensities of intermetallics affect the microhardness of the clad specimens. Higher intensity of intermetallics offered high resistance to indentation which resulted in increase in microhardness.

**Acknowledgements** This project is funded by the Science and Engineering Research Board (SERB), a statutory body of Department of Science and Technology (DST), Government of India under National Post-Doctoral Fellowship scheme (File No: PDF/2017/000412). The authors gratefully acknowledge the financial support by the DST-SERB, Government of India for this research work.

## References

1. Riquelme, A., Rodrigo, P., Escalera-Rodríguez, M.D., Rams, J.: Analysis and optimization of process parameters in Al–SiCp laser cladding. *Opt. Lasers Eng.* **78**, 165–173 (2016)
2. Kunjukunju, S., Roy, A., Ramanathan, M., Lee, B., Candiello, J.E., Kumta, P.N.: A layer-by-layer approach to natural polymer-derived bioactive coatings on magnesium alloys. *Acta Biomater.* **9**(10), 8690–8703 (2013)
3. Kirkland, N.T.: Magnesium biomaterials: past, present and future. *Corros. Eng. Sci. Technol.* **47**, 322–328 (2012)
4. Khalajabadi, S.Z., Bin Haji Abua, A., Ahmad, N., Azizi Mat Yajid, M., BtHjRedzuan, N., Nasiric, R., Haiderd, W., Noshadie, I.: Bio-corrosion behavior and mechanical characteristics of magnesium titania-hydroxyapatite nanocomposites coated by magnesium-oxide flakes and silicon for use as resorbable bone fixation material. *J. Mech. Behav. Biomed. Mater.* **77**, 360–374 (2018)
5. Liu, B., Zhang, X., Xiao, G.Y., Lu, Y.P.: Phosphate chemical conversion coatings on metallic substrates for biomedical application: a review. *Mater. Sci. Eng. C* **47**, 97–104 (2015)
6. Cui, Z., Yang, H., Wang, W., Wu, H., Xu, B.: Laser cladding Al-Si/Al<sub>2</sub>O<sub>3</sub>-TiO<sub>2</sub> composite coatings on AZ31B magnesium alloy. *J. Wuhan Univ. Technol. Mater. Sci. Ed.* **27**, 1042–1104 (2012)
7. Huang, K., Lin, X., Xie, C., Yue, T.M.: Laser cladding of Zr-based coating on AZ91D magnesium alloy for improvement of wear and corrosion resistance. *Bull. Mater. Sci.* **36**(1), 99–105 (2013)
8. Gao, Y., Wang, C., Lin, Q., Liu, H., Yao, M.: Broad-beam laser cladding of Al–Si alloy coating on AZ91HP magnesium alloy. *Surf. Coat. Technol.* **201**, 2701–2706 (2006)

9. Murr, L.E., Quinones, S.A., Gaytan, S.M., Lopez, M.I., Rodela, A., Martinez, E.Y., Hernandez, D.H., Martinez, E., Medina, F., Wicker, R.B.: Microstructure and mechanical behavior of Ti-6Al-4V produced by rapid-layer manufacturing, for biomedical applications. *J. Mech. Behav. Biomed. Mater.* **2**, 20–32 (2009)
10. Liu, S.Y., Hu, J.D., Yang, Y., Guo, Z.X., Wang, H.Y.: Microstructure analysis of magnesium alloy melted by laser irradiation. *Appl. Surf. Sci.* **252**, 1723–1731 (2005)